Controlling Localized Surface Plasmon Resonances in GeTe Nanoparticles Using an Amorphous-to-Crystalline Phase Transition

Mark J. Polking, Prashant K. Jain, Yehonadav Bekenstein, Uri Banin, Oded Millo, Ramamoorthy Ramesh, and A. Paul Alivisatos

Phys. Rev. Lett. **111**, 037401 — Published 16 July 2013

DOI: 10.1103/PhysRevLett.111.037401

Phase-Change Plasmonics with Colloidal Germanium Telluride Nanoparticles

Mark J. Polking,[1,†] *Prashant K. Jain,*[2] *Yehonadav Bekenstein,*[3,4] *Uri Banin,*[3] *Oded Millo,*[4,*] *Ramamoorthy Ramesh,*[1,5,*] *and A. Paul Alivisatos*[5,6,*]

[1]Department of Materials Science and Engineering, University of California, Berkeley, CA 94720, United States; [2]Department of Chemistry, University of Illinois, Urbana, IL 61801, United States; [3]Institute of Chemistry, The Hebrew University of Jerusalem, Jerusalem 91904, Israel; [4]Racah Institute of Physics, The Hebrew University of Jerusalem, Jerusalem 91904, Israel; [5]Materials Sciences Division, Lawrence Berkeley National Laboratory, Berkeley, CA 94720, United States; [6]Department of Chemistry, University of California, Berkeley, CA 94720, United States

[†]Present address: Department of Chemistry, Harvard University, Cambridge, MA 02138, United States

*To whom correspondence should be addressed: milode@mail.huji.ac.il; rramesh@berkeley.edu; alivis@berkeley.edu

Infrared absorption measurements of amorphous and crystalline nanoparticles of GeTe reveal a localized surface plasmon resonance (LSPR) mode in the crystalline phase that is absent in the amorphous. The LSPR mode emerges upon crystallization of amorphous nanoparticles. The contrasting plasmonic properties are elucidated with scanning tunneling spectroscopy measurements indicating a Burstein-Moss shift of the band gap in the crystalline phase and a finite density of electronic states throughout the bandgap in the amorphous phase that limits the effective free carrier density.

The emerging field of plasmonics represents a promising avenue towards realizing the confinement and control of light at sub-wavelength dimensions. The harnessing of *localized* surface plasmons confined to the surfaces of sub-wavelength metal particles in particular has found applications in fields including biosensing [1,2], optical antennas [3], and enhanced optical spectroscopy [4]. The breadth of applications has been hindered in part by the limited tunability of such localized surface plasmon resonance (LSPR) modes, which are fixed in traditional noble metal nanoparticles by the particle shape, size, carrier density, and surrounding dielectric environment [5,6]. Recent work [7-11] on LSPR modes in highly doped semiconductor nanocrystals, however, has enabled the *active* tuning of LSPR modes using chemical [7,8], optical [10], and electrical [11] stimuli via variation of the carrier density. The influences of both crystallographic and electronic structure on such resonances, however, remain largely unexplored, and methods for plasmon tuning compatible with integrated photonic devices are currently lacking. Here, we report the observation of a mid-infrared (MIR) LSPR mode in the phase-change semiconductor germanium telluride (GeTe), which undergoes rapid switching between amorphous and crystalline forms [12,13]. Both amorphous and crystalline GeTe

nanoparticles of similar size are prepared and plasmons are subsequently detected with Fourier transform infrared spectroscopy (FTIR). The prominent LSPR mode, present in the crystalline particles but absent in the amorphous, can be recovered in amorphous particles through rapid crystallization. These optical absorption measurements are consistent with the results of electrodynamic simulations performed using the Mie theory. The ability to switch GeTe between phases using either optical or electrical stimuli on nanosecond time scales opens the possibility of ultrafast, non-volatile control of plasmonic modes in a manner compatible with existing nanoelectronic and nanophotonic chips. The contrasting behavior of amorphous and crystalline samples is illuminated with scanning tunneling spectroscopy (STS) studies of individual nanoparticles of both forms, which reveal profound differences in electronic structure, manifested in a large Burstein-Moss shift of the band edge in the crystalline state and abundant deep trap levels in the amorphous form that reduce the effective free carrier density and quench the plasmon resonance. This work elucidates the role of physical and electronic structure on plasmonic properties and provides both a probe of this important phase transition and a potential route to ultrafast active plasmonic components that can be readily integrated with current device architectures.

Germanium telluride has been widely investigated for its applications in non-volatile phase-change memory devices [12,14] and its ferroelectric properties [15,16]. A semiconductor with a band gap of ~0.2 eV, bulk GeTe is highly non-stoichiometric with a density of Ge vacancies exceeding 10^{20} cm^{-3}, leading to a hole density on the order of 10^{21} cm^{-3}, comparable to that determined for plasmonic Cu_2S and Cu_2Se nanocrystals investigated previously [7,8,17].

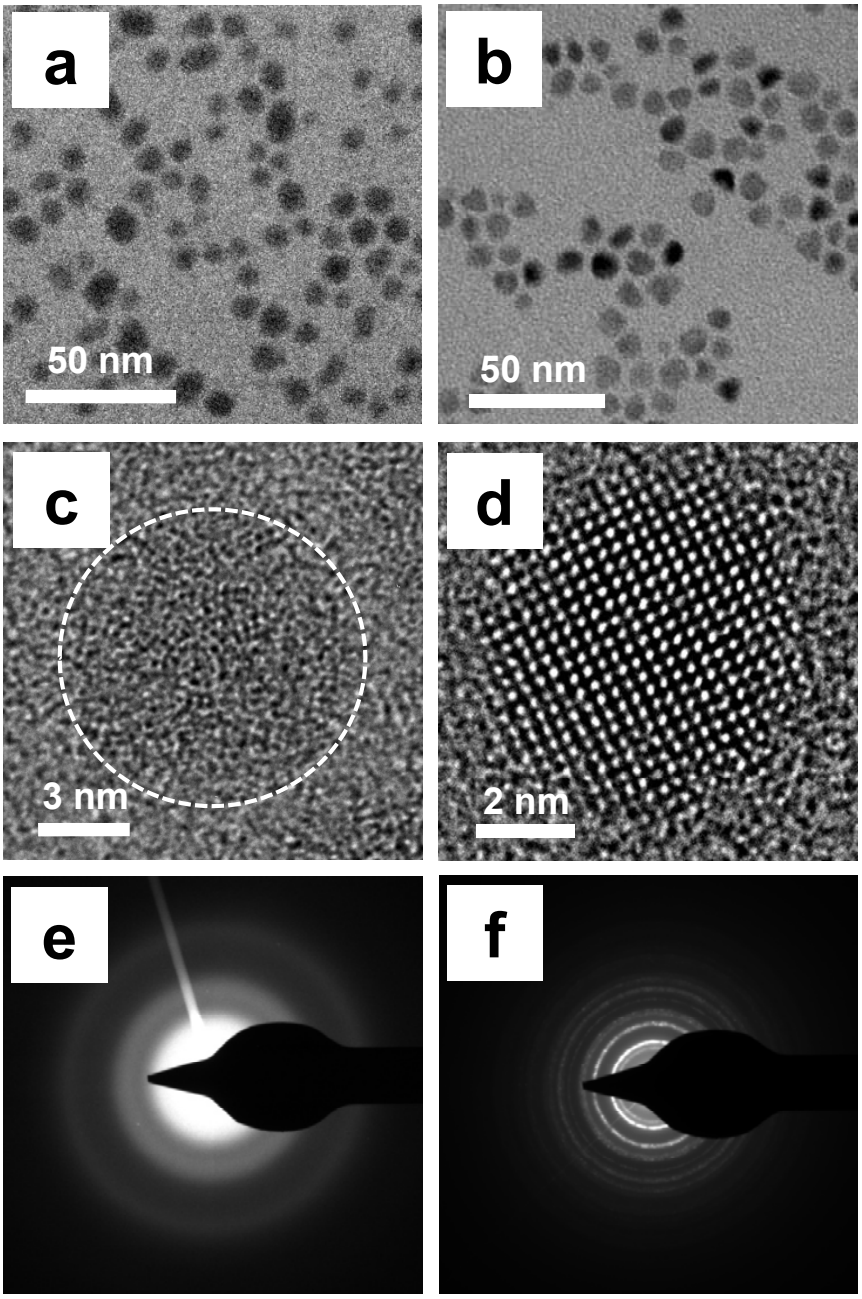

FIG. 1. Transmission electron microscope (TEM) images and electron diffraction patterns for amorphous and crystalline GeTe nanoparticles. (a, b) Low-resolution TEM images for amorphous (a) and crystalline (b) GeTe nanoparticles. (c, d) Typical high-resolution TEM images of amorphous (c) and crystalline (d) GeTe nanoparticles. The approximate area of the

amorphous particle in (c) is marked for clarity. (e, f) Selected-area electron diffraction patterns for amorphous (e) and crystalline (f) GeTe nanoparticles.

Nearly monodisperse GeTe nanoparticles have been prepared in both amorphous and crystalline forms previously using colloidal techniques [18-20]. The crystalline GeTe nanoparticles employed here were synthesized following a previous report [18], and the amorphous particles were prepared using a modification of this procedure. Details of the syntheses are provided in the Supplementary Material [21]. Nanoparticles of both phases were characterized structurally using transmission electron microscopy (TEM) and electron diffraction (ED) (Fig. 1). High-resolution TEM images of the amorphous particles (Fig. 1c) show minimal contrast and no lattice fringes, and ED patterns over a large area (Fig. 1e) reveal only very broad features, consistent with amorphous material. Characterization of the amorphous particles with energy-filtered TEM (see the Supplemental Material [21], Fig. S1) demonstrates uniform distribution of Ge and Te throughout the particles. *In-situ* crystallization of the amorphous particles in the TEM results in sharp diffraction features in the ED pattern (Fig. 1f), and TEM images (see the Supplemental Material [21], Fig. S2) indicate clear lattice fringes and crystallization into single domains.

Films of particles of both phases were characterized using FTIR in attenuated total reflectance (ATR) mode (Fig. 2). Poor solubility in the few solvents lacking strong IR absorption bands hindered measurements of particle solutions. The optical absorption spectrum of amorphous particles (Fig. 2a) reveals a gradual absorption onset beginning near ~0.3 eV and a series of sharp peaks near 0.35 eV from the C-H stretch of the 1-dodecanethiol ligands [22]. A broad feature between 0.4 and 0.45 eV attributable to the ligands is also evident. The absorption

spectrum of the crystalline particles (Fig. 2c), in contrast, includes a prominent, nearly Gaussian peak near ~0.5 eV with a linewidth of approximately 0.25 eV. This feature closely resembles the LSPR peaks observed previously for copper chalcogenide samples and is in strong agreement with the position of the free carrier absorption onset observed in bulk GeTe [23]. Temperature-dependent FTIR measurements (see the Supplemental Material [21], Fig. S3) show no significant changes in peak intensity or position from 80 to 300 K, inconsistent with excitonic absorption but consistent with the minimal temperature dependence of the free hole concentration and non-radiative plasmon damping in GeTe [17]. The proximity of this LSPR peak to the ligand features raises the possibility of coupling between plasmon modes and molecular vibrations.

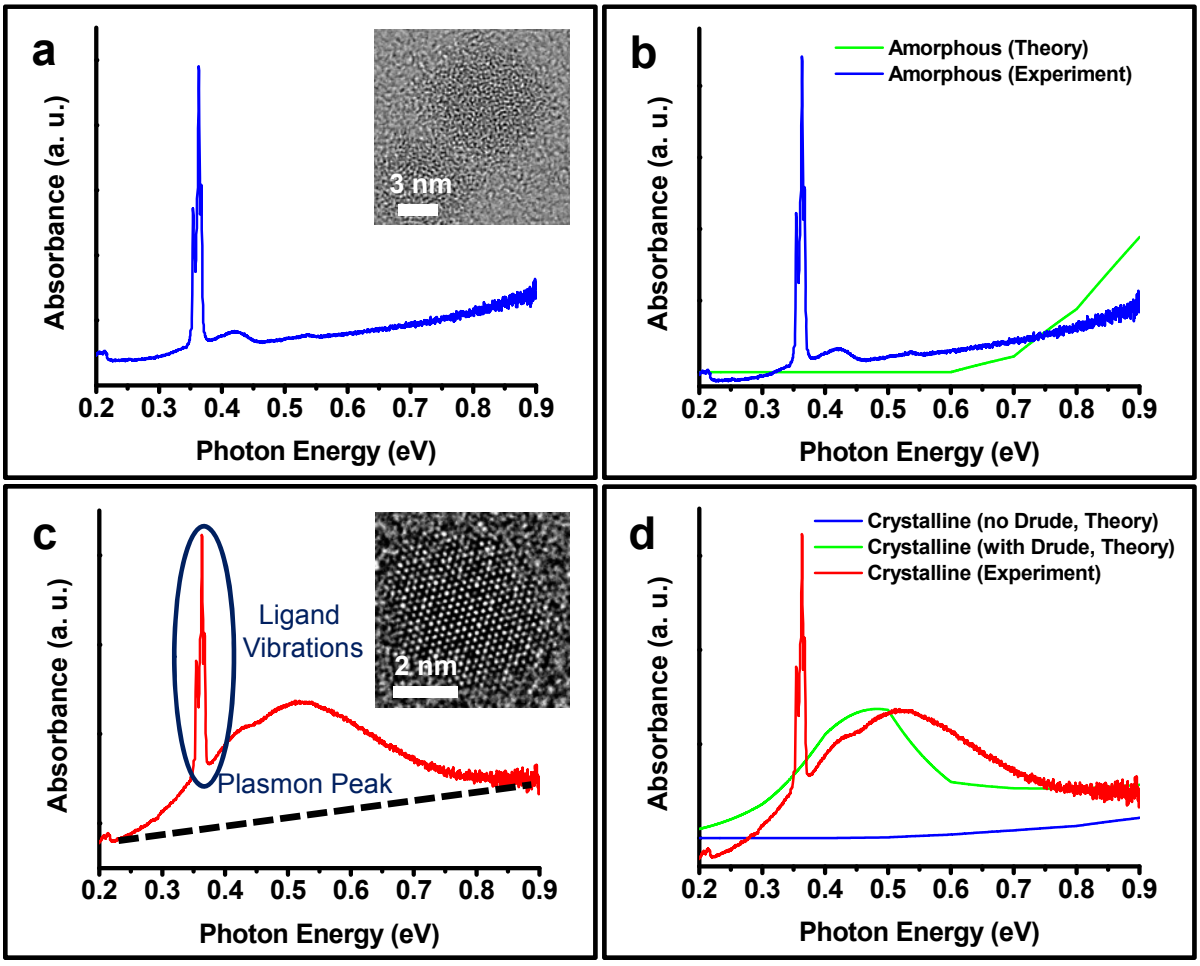

FIG. 2. Localized surface plasmon resonance (LSPR) in GeTe nanoparticles. (a) Fourier transform infrared (FTIR) absorption spectrum for amorphous GeTe nanoparticles. Inset: high-resolution TEM (HRTEM) image of an amorphous GeTe nanoparticle. (b) Comparison of an experimental extinction spectrum for amorphous GeTe nanoparticles with a theoretical spectrum calculated using the Mie theory. (c) FTIR absorption spectrum for crystalline GeTe nanoparticles illustrating a LSPR peak centered around ~0.5 eV. Inset: HRTEM image of a crystalline GeTe nanoparticle. (d) Comparison of an experimental extinction spectrum for crystalline GeTe nanoparticles with spectra calculated using the Mie theory. Strong agreement can be observed with the model including the Drude contribution. A molar absorption coefficient of 2.7×10^5 $M^{-1}cm^{-1}$ is estimated for the GeTe nanoparticles.

Evidence for the plasmonic origin of this feature can be obtained in part from electrodynamic calculations [24]. Calculations using the fully analytic Mie theory (Figs. 2b, 2d) performed with literature dielectric functions for GeTe [25] indicate pronounced differences between amorphous particles and crystalline particles modeled both with and without the Drude (free carrier) contribution. A medium refractive index of 1.45 was used to model the dodecanethiol ligand environment around the nanoparticles. For the amorphous particles (Fig. 2b), only a gradual absorption onset can be observed. Similar behavior is observed for the crystalline particles (Fig. 2d) without the Drude contribution, with the exception of a lower energy for the absorption onset. Inclusion of the Drude contribution with a free carrier density of 1.5×10^{21} cm^{-3}, however, results in the appearance of a prominent peak at ~0.5 eV with a linewidth of ~0.2 eV, in strong agreement with the experimental absorption spectrum. Our best-fit free carrier concentration is close to the range ($1.0\text{-}1.5 \times 10^{21}$ cm^{-3}) measured in past studies on GeTe [17], strengthening our LSPR assignment. No significant Drude contribution is present for amorphous GeTe [25].

Further evidence for the plasmonic origin of the absorption feature in Fig. 2c and a demonstration of potential for active plasmonic devices can be obtained through crystallization of amorphous nanoparticles. Films of amorphous nanoparticles were heated to 250 °C under argon for 20-60 seconds to induce crystallization and redispersed. Films measured prior to heating reveal an ATR-FTIR absorption spectrum matching that of Fig. 2a. Heating for increasing time intervals above the crystallization temperature (~145 °C in the bulk) [26] results in the gradual appearance of a nearly Gaussian absorption feature centered around ~0.45 eV with a linewidth of ~0.25 eV (Fig. 3), consistent with spectra for originally crystalline particles.

These experiments effectively rule out organic or other contaminants as a source for this feature and demonstrate phase-change switching of the LSPR mode. Measurement of the same batch of nanoparticles before and after crystallization also excludes stoichiometric differences as a source of the difference between material phases. The slow increase in LSPR absorption with crystallization time is likely attributable to slow heat diffusion through the substrate; *in-situ* crystallization experiments in the TEM described earlier allow crystallization with millisecond-scale heat pulses. Much faster switching of the LSPR mode is thus likely to be possible under appropriate conditions. Future ultrafast laser switching experiments may facilitate fast crystalline-to-amorphous phase switching and reversible on-off switching of the LSPR mode.

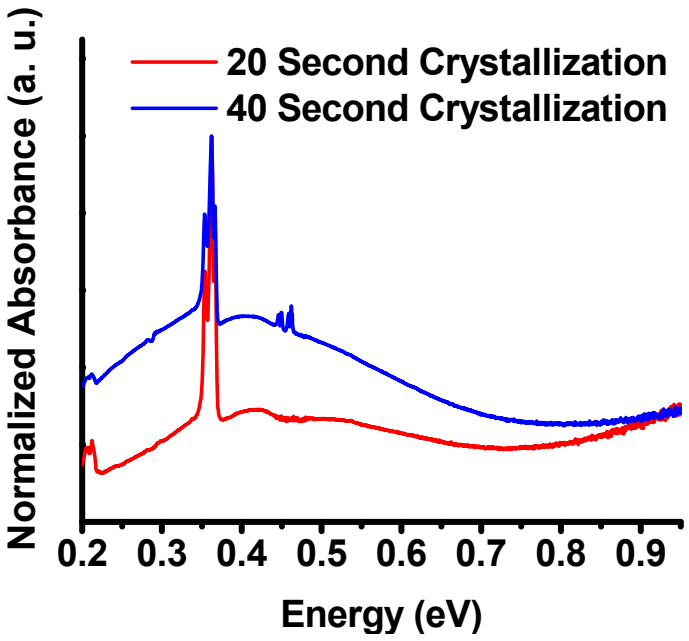

FIG. 3. Phase change-induced switching of the localized surface plasmon resonance (LSPR). The LSPR mode emerges as initially amorphous GeTe nanoparticles crystallize.

The origins of the contrasting plasmonic properties of amorphous and crystalline GeTe nanoparticles can be explored using STS, which provides a means of deciphering the density of states (DOS) in quantum dots and allows direct resolution of electronic wavefunctions [27]. STS measurements were performed with the tip positioned over individual amorphous and crystalline GeTe nanoparticles on Au(111) substrates (see the Supplemental Material [21], Figs. S4, S5) in a double barrier tunnel junction configuration [27-29]. When the tip is retracted such that the tunneling resistance across the tip-dot junction is greater, and the capacitance is smaller, than the resistance and capacitance across the dot-substrate junction, the tunneling conductance dI/dV vs. V accurately reflects the DOS of the dot [27,29]. STS spectra (Fig. 4) reveal pronounced differences in the DOS for the two particle types. STS spectra for the amorphous particles reveal a substantial finite DOS extending throughout the gap of approximately 1.0 eV. These spectra indicate that the amorphous GeTe particles retain the characteristic electronic structure of bulk amorphous material down to nanometer-level domain sizes. STS spectra for the same originally amorphous particles crystallized by heating under nitrogen, in contrast, show a well-defined band gap of approximately 0.4 eV without mid-gap states, substantially smaller than that for the amorphous particles.

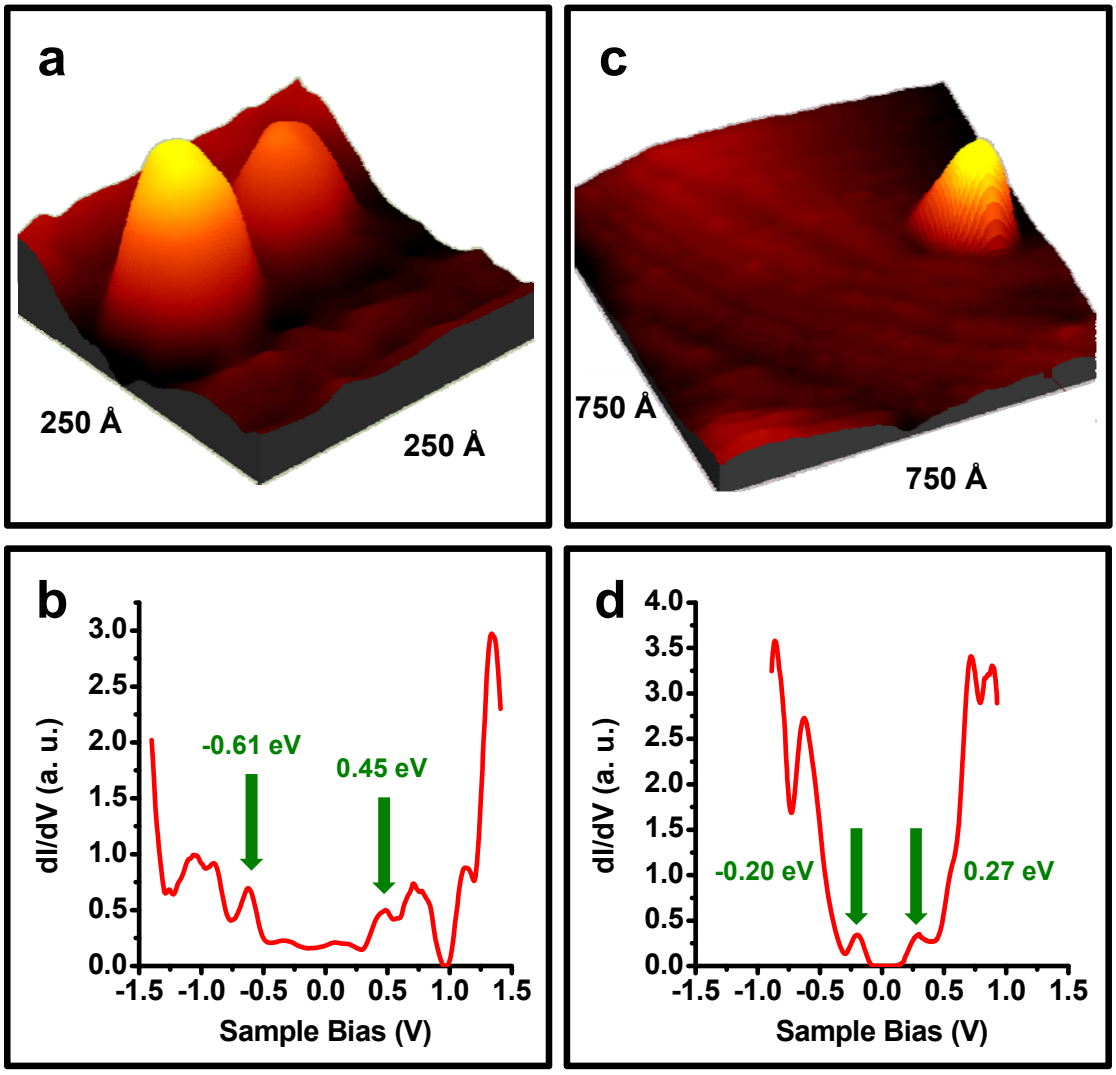

FIG. 4. Scanning tunneling spectroscopy of individual GeTe nanoparticles. (a, b) Topographic image (a) and plot of tunneling conductance vs. sample bias (b) for amorphous GeTe nanoparticles. In-gap states and a band gap of ~1 eV are observed. (c, d) Topographic image (c) and plot of tunneling conductance (d) for crystallized, originally amorphous GeTe nanoparticles. No in-gap states and a band gap of ~0.4 eV are observed.

Comparison of the STS spectra with optical absorption spectra demonstrates a significant difference in the apparent band gap for crystalline particles. For direct comparison between

optical spectra and STS data, the gap obtained from optical data must be corrected for the electron-hole Coulomb interaction by $1.8e^2/\varepsilon r$, in which ε is the dielectric constant and r the particle radius [27]. The corrected gap measured by optical means (~0.8 eV, see the Supplemental Material [21], Fig. S6) greatly exceeds that measured by STS, which ranged between 0.35 and 0.45 eV in the 7 crystalline particles measured. These data suggest a Fermi level lying approximately 0.4 eV inside the valence band, consistent with bulk GeTe with a hole density of ~10^{21} cm^{-3} [30]. This observation is consistent with the interpretation of the absorption feature in Fig. 2c as a LSPR mode and with Mie theory simulations. The Burstein-Moss shift is not observed in the STS spectra due to the cotunneling process in the double barrier tunnel junction. Here, electrons 'first' tunnel from the nanocrystal conduction band to the substrate, 'followed' by electron tunneling from the tip to the nanocrystal without violating the Pauli exclusion principle. The disappearance of the plasmon peak in the amorphous phase can be rationalized with reference to the DOS plot in Fig. 4c. The finite DOS in the gap provides abundant deep trap levels that limit the effective free carrier density. In addition, the observed electronic disorder can be expected to severely limit carrier mobilities, increasing the linewidth and completely damping a potential LSPR mode.

This work demonstrates the presence of a localized surface plasmon mode in colloidal GeTe nanocrystals. Switching of the LSPR is demonstrated through manipulation of the amorphous-crystalline phase transition. The presence (absence) of this LSPR mode is rationalized through scanning tunneling spectroscopy of crystalline (amorphous) particles. We observe a strong Burstein-Moss shift of the band gap for the crystalline phase due to degenerate p-type doping whereas extensive mid-gap states are seen in the amorphous phase that reduce the effective free carrier density. This work relates physical and electronic material structure to

plasmonic phenomena and provides a potential means of achieving rapid, non-volatile control of plasmons using thermal, electrical, or optical stimuli.

The authors acknowledge Hans Bechtel for assistance with FTIR measurements. Transmission electron microscopy at the National Center for Electron Microscopy was supported by the Office of Science, Office of Basic Energy Sciences, of the U.S. Department of Energy under contract No. DE-AC02-05CH11231. All other work was supported by the Physical Chemistry of Nanocrystals Project of the Director, Office of Science, Office of Basic Energy Sciences, of the U.S. Department of Energy under contract No. DE-AC02-05CH11231. M. J. P. was supported by a National Science Foundation (NSF) Graduate Research Fellowship and a NSF Integrative Graduate Education and Research Traineeship fellowship.

[1] C. Sönnichsen, B. M. Reinhard, J. Liphardt, and A. P. Alivisatos, Nat. Biotechnol. **23,** 741 (2005).

[2] J. N. Anker, W. Paige Hall, O. Lyandres, N. C. Shah, J. Zhao, and R. P. Van Duyne, Nat. Mater. **7,** 442 (2008).

[3] M. W. Knight, H. Sobhani, P. Nordlander, and N. J. Halas, Science **332,** 702 (2011).

[4] S. Nie and S. R. Emory, Science **275,** 1102 (1997).

[5] K. L. Kelly, E. Coronado, L. L. Zhao, and G. C. Schatz, J. Phys. Chem. B **107,** 668 (2003).

[6] M. A. El-Sayed, Acc. Chem. Res. **34,** 257 (2001).

[7] J. M. Luther, P. K. Jain, T. Ewers, and A. P. Alivisatos, Nat. Mater. **10,** 361 (2011).

[8] D. Dorfs, T. Härtling, K. Miszta, N. C. Bigall, M. R. Kim, A. Genovese, A. Falqui, M. Povia, and L. Manna, J. Am. Chem. Soc. **133,** 11175 (2011).

[9] K. Manthiram and A. P. Alivisatos, J. Am. Chem. Soc. **134,** 3995 (2012).

[10] F. Scotognella, G. Della Valle, A. R. S. Kandada, D. Dorfs, M. Zavelani-Rossi, M. Conforti, K. Miszta, A. Comin, K. Korobchevskaya, G. Lanzani, L. Manna, and F. Tassone, Nano Lett. **11,** 4711 (2011).

[11] G. Garcia, R. Buonsanti, E. L. Runnerstrom, R. J. Mendelsberg, A. Llordes, A. Anders, T. J. Richardson, and D. J. Milliron, Nano Lett. **11,** 4415 (2011).

[12] D. Yu, J. Wu, Q. Gu, and H. Park, J. Am. Chem. Soc. **128,** 8148 (2006).

[13] G. Bruns, P. Merkelbach, C. Schlockermann, M. Salinga, M. Wuttig, Appl. Phys. Lett. **95,** 043108 (2009).

[14] R. G. D. Jeyasingh, M. A. Caldwell, D. J. Milliron, and H.-S. Philip Wong in *Proceedings of the European Solid-State Device Research Conference, Helsinki (2011)* p. 99.

[15] M. J. Polking, J. J. Urban, D. J. Milliron, H. Zheng, E. Chan, M. A. Caldwell, S. Raoux, C. F. Kisielowski, J. W. Ager III, R. Ramesh, and A. P. Alivisatos, Nano Lett. **11,** 1147 (2011).

[16] E. F. Steigmeier and G. Harbeke, Solid State Commun. **8,** 1275 (1970).

[17] S. K. Bahl and K. L. Chopra, J. Appl. Phys. **41,** 2196 (1970).

[18] M. J. Polking, H. Zheng, R. Ramesh, and A. P. Alivisatos, J. Am. Chem. Soc. **133,** 2044 (2011).

[19] M. A. Caldwell, S. Raoux, R. Y. Wang, H.-S. Philip Wong, and D. J.Milliron, J. Mater. Chem. **20,** 1285 (2010).

[20] I. U. Arachchige, R. Soriano, C. D. Malliakas, S. A. Ivanov, and M. G. Kanatzidis, Adv. Mater. **21,** 2737 (2011).

[21] See Supplemental Material at [URL] for details on the experimental methods and for supplemental figures including additional transmission electron microscope, atomic force microscope, scanning tunneling microscope, and optical absorption data.

[22] *Spectral Database for Organic Compounds (SDBS)*; IR spectrum; SDBS No.: 10643; RN 112-55-0; http://riodb01.ibase.aist.go.jp/sdbs/cgi-bin/direct_frame_top.cgi (accessed November 16, 2012).

[23] R. Tsu, W. E. Howard, and L. Esaki, Solid State Commun. **5,** 167 (1967).

[24] P. K. Jain, K.-S. Lee, I. H. El-Sayed, and M. A. El-Sayed, J. Phys. Chem. B **110,** 18243 (2006).

[25] K. Shportko, S. Kremers, M. Woda, D. Lencer, J. Robertson, and M. Wuttig, Nat. Mater. **7,** 653 (2008).

[26] K. L. Chopra and S. K. Bahl, J. Appl. Phys. **40,** 4171 (1969).

[27] U. Banin and O. Millo, Annu. Rev. Phys. Chem. **54,** 465 (2003).

[28] A. E. Hanna and M. Tinkham, Phys. Rev. B **44,** 5919 (1991).

[29] E. P. A. M. Bakkers and D. Vanmaekelbergh, Phys. Rev. B **62,** 7743 (2000).

[30] S. K. Bahl and K. L. Chopra, J. Appl. Phys. **40,** 4940 (1969).